

N IV EMISSION LINES IN THE ULTRAVIOLET SPECTRA OF GASEOUS NEBULAE

F. P. KEENAN

Department of Pure and Applied Physics, The Queen's University of Belfast, Belfast BT7 1NN, Northern Ireland, UK

C. A. RAMSBOTTOM, K. L. BELL, K. A. BERRINGTON, AND A. HIBBERT

Department of Applied Mathematics and Theoretical Physics, The Queen's University of Belfast,
Belfast BT7 1NN, Northern Ireland, UKW. A. FEIBELMAN¹Laboratory for Astronomy and Solar Physics, Code 684.1, NASA-Goddard Space Flight Center,
Greenbelt, MD 20771

AND

W. P. BLAIR

Center for Astrophysical Sciences, Department of Physics and Astronomy,
The Johns Hopkins University, Baltimore, MD 21218

Received 1994 May 3; accepted 1994 July 5

ABSTRACT

Theoretical electron density sensitive emission-line ratios, determined using electron impact excitation rates calculated with the *R*-matrix code, are presented for $R = I(2s^2\ ^1S-2s2p\ ^3P_2)/I(2s^2\ ^1S-2s2p\ ^3P_1) = I(1483\ \text{\AA})/I(1486\ \text{\AA})$ in N IV. These are found to be up to an order of magnitude different from those deduced by previous authors, principally due to the inclusion of excitation rates for transitions among the $2s2p\ ^3P$ fine-structure levels. The observed values of *R* for several planetary nebulae, symbiotic stars and the Cygnus Loop supernova remnant, measured from spectra obtained with the *International Ultraviolet Explorer (IUE)* satellite and the *Hopkins Ultraviolet Telescope (HUT)*, lead to electron densities which are in excellent agreement with those deduced from line ratios in other species. This provides observational support for the accuracy of the atomic data adopted in the present calculations.

Subject headings: atomic data — atomic processes — ultraviolet: ISM

1. INTRODUCTION

The forbidden ($J = 2$) and intercombination ($J = 1$) components of the $2s^2\ ^1S-2s2p\ ^3P_J$ multiplet in N IV have been observed at wavelengths of ~ 1483 and $\sim 1486\ \text{\AA}$, respectively, in the ultraviolet spectra of low-density astrophysical plasmas, such as planetary nebulae and symbiotic stars (Feibelman, Aller, & Hyung 1992; Doschek & Feibelman 1993). These transitions, which are analogous to the well-known 1907 and 1909 \AA line pair in C III (Keenan, Feibelman, & Berrington 1992a), may be used to derive the electron density (N_e) of the emitting plasma through their emission-line ratio, $R = I(1483\ \text{\AA})/I(1486\ \text{\AA})$. Several calculations of *R* have been performed, the most recent being those by Czyzak, Keyes, & Aller (1986), which employed electron impact excitation rates for the $2s^2\ ^1S-2s2p\ ^3P_J$ transitions that had been interpolated from existing data for C III and O V (Mendoza 1983).

Very recently, Ramsbottom et al. (1994) have calculated electron excitation rates in N IV using the *R*-matrix method as adapted for the Opacity Project (Seaton 1987; Berrington et al. 1987) and found results significantly different from those of Mendoza (1983). For example, at $T_e = 5000\ \text{K}$, the Ramsbottom et al. (1994) rate for $2s^2\ ^1S-2s2p\ ^3P_1$ is a factor of 1.8 larger than that of Mendoza, while at $T_e = 10,000\ \text{K}$, the *R*-matrix data are $\sim 40\%$ larger. In this paper we use the Ramsbottom et al. (1994) results to derive *R* ratios applicable to gaseous

nebulae, and compare these with observations obtained with both the *International Ultraviolet Explorer (IUE)* satellite and the *Hopkins Ultraviolet Telescope (HUT)*.

2. THEORETICAL RATIOS

The model ion for N IV consisted of the six energetically lowest LS states, namely $2s^2\ ^1S$; $2s2p\ ^3P$, 1P ; $2p^2\ ^3P$, 1D and 1S , making a total of 10 fine-structure levels. Energies for all these levels were taken from Moore (1965).

Electron impact excitation for transitions in N IV were taken from the 12 state calculation of Ramsbottom et al. (1994), while for Einstein *A*-coefficients the calculations of Nussbaumer & Storey (1979) were adopted, apart from the important $2s^2\ ^1S-2s2p\ ^3P_1$ intercombination line, where the transition probability of Glass & Hibbert (1978) was preferred. (We note in passing that the Nussbaumer & Storey *A*-values alone were used by Czyzak et al. (1986) in their N IV diagnostic calculations). Proton impact excitation rates, which are only important for transitions within $2s2p\ ^3P$ (Seaton 1964), were taken from Doyle (1987).

Using the atomic data discussed above in conjunction with the statistical equilibrium code of Dufton (1977), relative N IV level populations and hence emission-line strengths were calculated for a range of electron temperatures and densities. The following assumptions were made in the calculations. (1) that photoexcitation and deexcitation rates are negligible in comparison with the corresponding collisional rates, (2) that ionization to and recombination from other ionic levels is slow compared with bound-bound rates, and (3) that all transitions are optically thin. Further details of the procedures involved may be found in Dufton (1977) and Dufton et al. (1978).

¹ Guest observer with the *International Ultraviolet Explorer* satellite, which is operated and sponsored by the National Aeronautics and Space Administration, by the European Space Agency, and by the Science and Engineering Research Council of the United Kingdom.

In Figure 1, we plot the theoretical ratio

$$R = I(2s^2\ ^1S - 2s2p\ ^3P_2)/I(2s^2\ ^1S - 2s2p\ ^3P_1) \\ = I(1483\ \text{\AA})/I(1486\ \text{\AA})$$

as a function of electron density for three electron temperatures, namely $T_e = 5000, 10,000,$ and $20,000$ K. An inspection of the figure reveals the potential usefulness of the ratio as an electron density diagnostic, as it varies strongly with density for $N_e \geq 10^4\ \text{cm}^{-3}$, but is quite insensitive to electron temperature. For example, at $T_e = 10,000$ K, R varies by a factor of ~ 16 between $N_e = 10^4$ and $10^6\ \text{cm}^{-3}$. However, the change in the ratio between $T_e = 10,000$ and $20,000$ K is only $\sim 2\%$ at $N_e = 10^4\ \text{cm}^{-3}$, and $\sim 37\%$ at $N_e = 10^6\ \text{cm}^{-3}$.

Also shown in Figure 1 are the theoretical R ratios of Czyzak et al. (1986) at $T_e = 10,000$ K. An inspection of the figure reveals that our results for R are significantly different from those of Czyzak et al., being $\sim 20\%$ smaller than $N_e = 10^4\ \text{cm}^{-3}$, and a factor of ~ 10 lower at $N_e = 10^6\ \text{cm}^{-3}$. These discrepancies are not primarily due to the adoption of improved atomic data for the $2s^2\ ^1S-2s2p\ ^3P$ lines in the present analysis, but rather because we have included excitation rates for the $2s2p\ ^3P_J-2s2p\ ^3P_J$ transitions, which were not considered by Czyzak et al., as data for these were not given in the compilation of Mendoza (1983). However, we should point out that Czyzak et al. were aware of the need to include rates among the $2s2p\ ^3P$ levels for the reliable determination of theoretical emission-line ratios, from their work on the analogous $3s^2\ ^1S-3s3p\ ^3P$ multiplet in Si III (see also Keenan et al. 1992b and Johnson, Smith, & Parkinson 1986 for similar results on Al II).

3. OBSERVATIONAL DATA

Observed values of R have been measured from high-resolution ultraviolet spectra obtained with *IUE* satellite. The objects considered (a sample of three planetary nebulae and four symbiotic stars) are listed in Table 1, along with the *IUE*

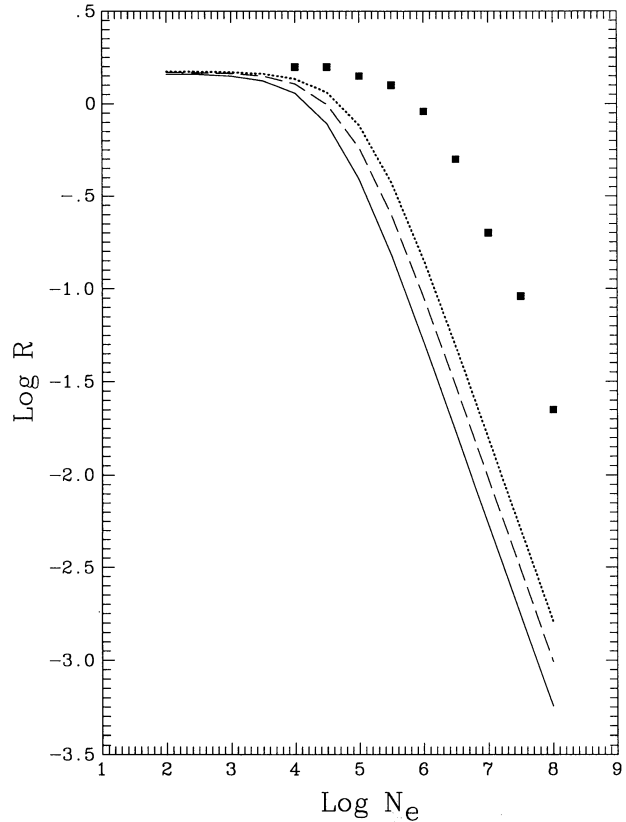


FIG. 1.—The theoretical N IV emission-line ratio $R = I(2s^2\ ^1S-2s2p\ ^3P_2)/I(2s^2\ ^1S-2s2p\ ^3P_1) = I(1483\ \text{\AA})/I(1486\ \text{\AA})$, plotted as a function of logarithmic electron density (N_e in cm^{-3}). The present calculations are shown in electron temperatures of $T_e = 5000$ K (solid line), $10,000$ K (dashed line), and $20,000$ K (dotted line), while the results of Czyzak et al. (1986) are plotted at $T_e = 10,000$ K (solid squares).

TABLE 1
OBSERVED N IV LINE INTENSITY RATIOS AND DERIVED LOGARITHMIC ELECTRON DENSITIES

OBJECT	SWP IMAGE NUMBER	R	T_e (K)	$\log N_e(R)$		
				Present Results	Czyzak et al. 1986	$\log N_e(\text{other})$
Planetary nebula						
NGC 3918	21764	1.60	12500 ^a	≤ 3.0	≤ 4.0	3.0 ^b
IC 4997	41093	0.57	12500 ^c	5.3	6.6	5.0 ^c
Hu 1-2	44662	0.61	10000 ^d	4.5	6.4	4.7 ^d
Symbiotic stars						
RR Tel	20246	0.05	13000 ^e	6.2	7.5	6.4 ^e
V1016 Cyg	13432	0.05	25000 ^f	6.5	7.7	6.4 ^g
AX Per	21443	0.09	12000 ^h	6.0	7.2	5.7 ^h
HM Sge	30081	0.11	17500 ^f	6.2	7.2	6.2 ^f
Supernova remnant						
Cygnus Loop	HUT	1.56	12400 ⁱ	≤ 3.0	≤ 4.0	1.6 ⁱ

^a Kaler 1986.

^b Keenan et al. 1992a.

^c Hyung, Aller, & Feibelman 1994.

^d Rudy et al. 1993.

^e Hayes & Nussbaumer 1986.

^f Schmid & Schild 1990.

^g Feibelman 1982.

^h Nussbaumer et al. 1988.

ⁱ Raymond et al. 1988.

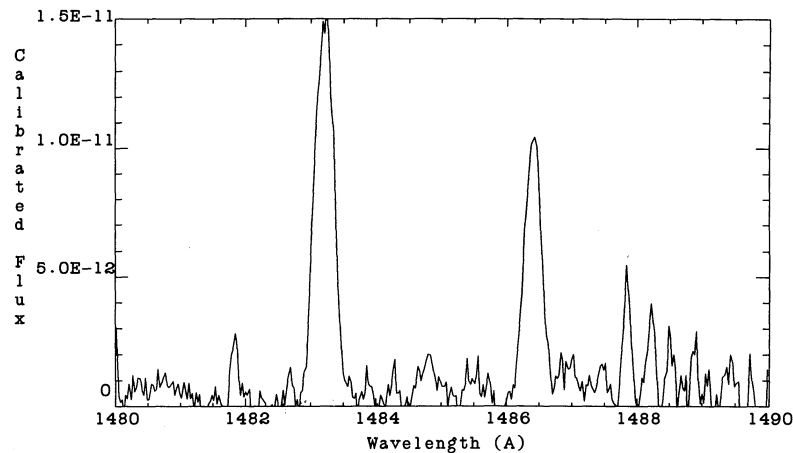


FIG. 2.—High-resolution *IUE* spectrum (SWP 21764) of the planetary nebula NGC 3918 in the wavelength region 1480–1490 Å, where the flux is in units of $\text{ergs cm}^{-2} \text{s}^{-1}$. The N IV lines at 1483 and 1486 Å are clearly visible in the spectrum.

images used in the analysis. Also given are the derived R ratios, which were determined using software at the *IUE* Data Analysis Center. The spectra of one planetary nebula (NGC 3918) and one symbiotic star (V1016 Cyg) are shown in Figures 2 and 3, respectively, to illustrate the quality of the observational data.

We have also measured the value of R in the spectrum of the Cygnus Loop supernova remnant, obtained by the *HUT* during the *Astro-1* space shuttle mission in 1990 December, as described in Blair et al. (1991). *HUT* consists of a 0.9 m mirror that feeds a prime focus spectrograph with a microchannel plate intensifier and Reticon detector. First-order sensitivity covers the wavelength region from 850 to 1850 Å at 0.5 Å pixel^{-1} with point source resolution of $\sim 3 \text{ Å}$. Details of the spectrograph, telescope and calibration may be found in Davidsen et al. (1992).

The data published by Blair et al. (1991) constituted only the last 638 s out of a 1902 s observation; this was the portion of data obtained during orbital night. However, the spectral region around the N IV lines is nearly uncontaminated by residual airglow emissions, with the exception of two faint N I transitions at 1492.6 and 1494.7 Å. Hence, we have reprocessed

the entire dataset for use in this paper. The region of the resulting *HUT* spectrum containing the N IV lines is shown in Figure 4.

Because the *HUT* resolution is on a par with the line separation, we have derived the value of R by careful profile fitting of the *HUT* spectrum. Since the *HUT* detector is photon-counting, a detailed error array can be constructed and carried throughout the data reduction process. This information is used with a program called “Specfit” (written by G. A. Kriss at Johns Hopkins) to fit *Gaussian* profiles to the lines and minimize chi-squared to obtain the best fit to the data. For the N IV lines, the relative wavelengths were fixed in the proper ratio and the lines were forced to have the same line width. The fits to the N IV line profiles are shown in Figure 4, while the resulting value of R is given in Table 1.

4. RESULTS AND DISCUSSION

In Table 1 we summarize the electron densities derived from the observed values of R , denoted $\log N_e(R)$, using both the calculations in Figure 1 and the diagnostics of Czyzak et al. (1986), along with the adopted electron temperatures from the

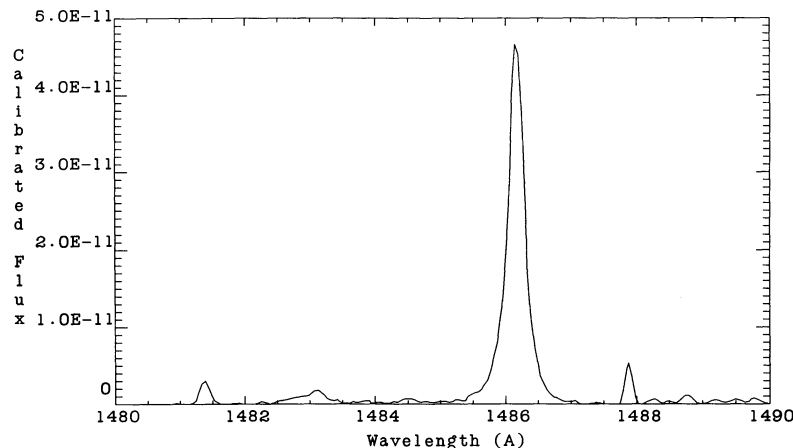


FIG. 3.—High-resolution *IUE* spectrum (SWP 13432) of the symbiotic star V1016 Cyg in the wavelength region 1480–1490 Å, where the flux is in units of $\text{ergs cm}^{-2} \text{s}^{-1}$. The N IV lines at 1483 and 1486 Å are clearly visible in the spectrum.

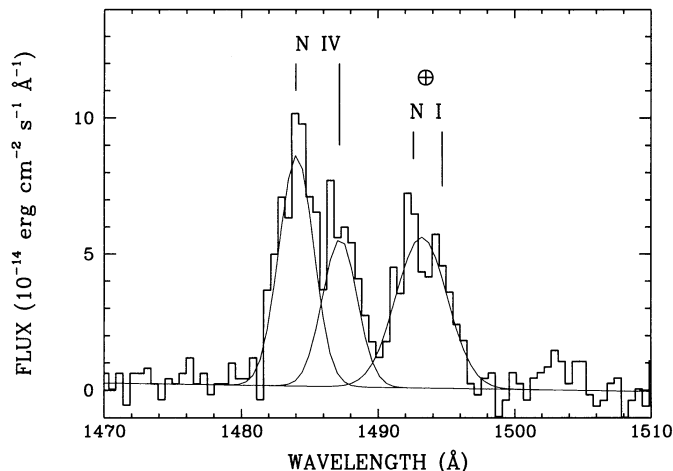


FIG. 4.—HUT spectrum of the Cygnus Loop supernova remnant in the 1470–1510 Å wavelength range. The histogram shows the observational data, while the smooth curves are the fits to both the N IV 1483 and 1486 Å lines and the N I 1492.6 and 1494.7 Å airglow features (marked by ⊕). The latter were modeled using a single Gaussian.

references given as footnotes. Also listed in the table are the electron densities, designated $\log N_e(\text{other})$, derived from line ratios in species with similar ionization potentials (and hence spatial distributions) to N IV, such as $I(1407 \text{ \AA})/I(1402 \text{ \AA})$ in O IV. An inspection of the table reveals that the electron densities estimated from the line ratio calculations in Figure 1 are typically a factor of ~ 20 smaller than those derived using

the Czyzak et al. results. However, the former are in far better agreement with the densities deduced from line ratios in other species. This is illustrated by the quantity $|\log N_e(R) - \log N_e(\text{other})|$, i.e., the magnitude of the difference between the densities deduced from R and from other line ratios, which averages ~ 1.4 dex for the Czyzak et al. calculations, but only ~ 0.2 dex for the current diagnostics.

The good agreement found between densities determined from the present N IV line ratios and those inferred from other species provides experimental support for the accuracy of the former, and hence for the atomic data used in their derivation. Further support for the atomic data comes from the IUE and HUT observations of NGC 3818 and Cygnus Loop, respectively. In these objects, the electron densities are small enough for R to be in its low-density limit (i.e., $N_e \leq 10^3 \text{ cm}^{-3}$ from Fig. 1), and hence in the coronal approximation (Elwert 1952), so that the theoretical value of R will depend only on the magnitude of the relevant electron excitation rates and the Einstein A -coefficient of the $2s2p^3P_1 - 2s2p^3P_2$ transition (Dufton, Keenan, & Kingston 1984). For both NGC 3918 and the Cygnus Loop, the observed values of $R \simeq 1.6$, which only differ from the theoretical result by $\sim 7\%$, hence providing further verification of the atomic data.

We would like to thank G. A. Warren for help with the preparation of Figure 1. The IUE archival portion of this work was supported by the IUE Data Analysis Center (IUEDAC). This work was financially supported by NATO travel grant CRG.930722 and the Royal Society.

REFERENCES

- Berrington, K. A., Burke, P. G., Butler, K., Seaton, M. J., Storey, P. J., Taylor, K. T., & Yu, Y. 1987, *J. Phys. B*, 20, 6379
 Blair, W. P., et al. 1991, *ApJ*, 379, L33
 Czyzak, S. J., Keyes, C. D., & Aller, L. H. 1986, *ApJS*, 61, 159
 Davidsen, A. F., et al. 1992, *ApJ*, 392, 264
 Doschek, G. A., & Feibelman, W. A. 1993, *ApJS*, 87, 331
 Doyle, J. G. 1987, *Atom. Data Nucl. Data Tables*, 37, 441
 Dufton, P. L. 1977, *Comput. Phys. Comm.*, 13, 25
 Dufton, P. L., Berrington, K. A., Burke, P. G., & Kingston, A. E. 1978, *A&A*, 62, 111
 Dufton, P. L., Keenan, F. P., & Kingston, A. E. 1984, *MNRAS*, 209, 1P
 Elwert, G. 1952, *Z. Nat.*, 7A, 432
 Feibelman, W. A. 1982, *ApJ*, 258, 548
 Feibelman, W. A., Aller, L. H., & Hyung, S. 1992, *PASP*, 104, 339
 Glass, R., & Hibbert, A. 1978, *J. Phys. B*, 11, 2413
 Hayes, M. A., & Nussbaumer, H. 1986, *A&A*, 161, 287
 Hyung, S., Aller, L. H., & Feibelman, W. A. 1994, *ApJS*, in press
 Johnson, B. C., Smith, P. L., & Parkinson, W. H. 1986, *ApJ*, 308, 1013
 Kaler, J. B. 1986, *ApJ*, 308, 322
 Keenan, F. P., Feibelman, W. A., & Berrington, K. A. 1992a, *ApJ*, 389, 443
 Keenan, F. P., Harra, L. K., Aggarwal, K. M., & Feibelman, W. A. 1992b, *ApJ*, 385, 375
 Mendoza, C. 1983, in *IAU Symp. 103, Planetary Nebulae*, ed. D. R. Flower (Dordrecht: Reidel), 143
 Moore, C. E. 1965, *Atomic Energy Levels*, NSRDS-NBS35
 Nussbaumer, H., Schild, H., Schmid, H. M., & Vogel, M. 1988, *A&A*, 198, 179
 Nussbaumer, H., & Storey, P. J. 1979, *A&A*, 74, 244
 Ramsbottom, C. A., Berrington, K. A., Hibbert, A., & Bell, K. L. 1994, *Phys. Scripta*, in press
 Raymond, J. C., Herter, J. J., Cox, D., Blair, W. P., Fesen, R. A., & Gull, T. R. 1988, *ApJ*, 324, 869
 Rudy, R. J., Rossano, G. S., Erwin, P., Puetter, R. C., & Feibelman, W. A. 1993, *AJ*, 105, 1002
 Schmid, H. M., & Schild, H. 1990, *MNRAS*, 246, 84
 Seaton, M. J. 1964, *MNRAS*, 127, 191
 ———. 1987, *J. Phys. B*, 20, 6363